Layer-by-Layer Assembly of Polyoxometalates into Microcapsules

Lei Gao, Enbo Wang,* Zhenhui Kang, Yanli Song, Baodong Mao, and Lin Xu

Polyoxometalate Institute, Chemistry Department, Northeast Normal University, Changchun, Jilin, People's Republic of China 130024

Received: April 8, 2005; In Final Form: May 31, 2005

The polyoxometalate (POM) chemistry world has been experiencing an unparalleled development of rapid synthesis of new compounds and slow development of POM-based functional materials and devices. Meanwhile, researchers in the microcapsule world, encouraged by the introduction of the layer-by-layer method, are pursuing good components for constructing functional capsule devices. Here, in view of the versatile properties that POM-based microcapsules may possess, various types of POM−polyelectrolyte composite microcapsules were constructed using the layer-by-layer method. Microscopy reveals that polyoxometalates form nanoparticles on the shell in the presence of cationic polyelectrolytes. These nanoparticles connected with polyelectrolytes constitute the shell and support the microcapsule from collapse after drying, and this is an interesting characteristic different from those of common composite and polyelectrolyte capsules. Fourier transform infrared (FTIR), UV−vis absorption, and X-ray photoelectron spectroscopy (XPS) were used to examine the properties of the POMs in the microcapsules. The obtained microcapsules exhibit higher thermal stability than polyelectrolyte microcapsules. Furthermore, the functions of POMs were maintained when they were assembled into microcapsules. It is proved that microcapsules bearing POMs with redox activity can provide a reduction environment, which can lead to the realization of in situ synthesis of materials, and that microcapsules with photoluminescent POMs as a component can also have a photoluminescent property, providing a way to develop functional capsule devices. This work may provide an opportunity to enrich both the polyoxometalate chemistry and the capsule field.

Introduction

Early transition metal polyoxometalates represent a well-known class of structurally well-defined clusters which are known to have an extensive surface chemistry that plays a key role in various areas such as catalysis,[1−3] corrosion protection,[4,5] and electrochemistry.[6−9] As early as 1998, Klemperer and Wall reviewed and predicted that the future of polyoxometalate chemistry would finally move from solids and solutions to surfaces.[10] Numerous examples have emerged and fully supported this idea. Polyoxometalates were successfully deposited on metal surfaces, electrode surfaces, and then macroscopic flat quartz surfaces, which quickly made POM-based inorganic−organic composite films[11−16] a great research interest in materials engineering science. However, polyoxometalate chemistry is still experiencing unparalleled development of rapid synthesis of functional POM-based new compounds and slow development of functional materials and devices.[13] Recently, some new efforts are devoted to exploring POM-based nanostructures,[17−19] and a recent study reported an interesting polyoxometalate-based vesicle and its honeycomb architectures on solid surfaces.[20] All these studies provide a spark to the development of polyoxometalate-based functional devices. However, further exploring new application fields and developing POM-based functional devices still pose a challenge for polyoxometalate chemists.

Recently, the investigation of organic−inorganic composite materials has become a rapidly developing and expanding area with great potential for industrial application. The possibility of combining different characteristics of the components to achieve synergistic and hybrid effects, and the main advantages of such materials in their physical, chemical, and biomedical properties, have made studies of this specific field extremely significant.

On the basis of electrostatic interactions, the layer-by-layer technique provides a convenient way to realize the construction of inorganic−organic composite materials, because it can easily render organic and inorganic species with opposite charges assembled into composite bilayers. Recently, this technique has been explored in an effort to fabricate inorganic−organic hollow capsules. Hollow capsules with nanometer to micrometer dimensions constitute an important class of materials that are employed in various technological aspects, ranging from the delivery of encapsulated products for cosmetic and medicinal purposes to their use as lightweight composite materials and as fillers with a low dielectric constant in electronic components.[21] Until now, many organic−inorganic composite capsules with interesting functions have been synthesized using the layer-by-layer method. Typical examples include assembling SiO_2,[22] TiO_2,[23] and Fe_3O_4[24] nanoparticles, carboxylated multiwalled carbon nanotubes,[25] and multivalent ions[26] onto core particles which subsequently decompose. The composite microcapsules that were obtained were proved to bear multifunctions derived from both the organic and inorganic components. Shchukin et al. has found that polyelectrolyte microcapsules modified with Fe_3O_4 nanoparticles not only maintained the selective permeability of common polyelectrolyte capsules but also could be used as protective microcontainers capable of preventing encapsulated compounds from being oxidized by low-molecular weight oxidizing agents.[24]

* To whom correspondence should be addressed. E-mail: wangenbo@public.cc.jl.cn. Fax: +86-431-5098787.

10.1021/jp051818f CCC: $30.25
Published on Web 08/17/2005

At present, polyoxometalate chemistry represents an undeveloped field in this microcapsule world. If properly positioning POMs on micrometer-scale surfaces and maintaining their individual unique properties, a new material engineering field would be created, in which the diverse functions of numerous polyoxometalates and those of microcapsules could be well combined, thus opening a new way to develop POM-based functional devices. In view of such a possibility, different POMs were assembled into microcapsules employing the layer-by-layer method in this work, and POM-based inorganic−inorganic composite microcapsules were obtained. As Kurth et al. once pointed out, the realization of POM-based materials will require new methods for combining, positioning, and orienting the clusters in the device architecture.[25] Meanwhile, all the applications microcapsules may possess are closely related to the properties of the shell. This work may then provide a good way of enriching both polyoxometalate chemistry and the microcapsule world.

Experimental Section

Materials. Poly(allylamine hydrochloride) (PAH, MW ≈ 70 000) and sodium poly(styrene sulfonate) (PSS, MW ≈ 70 000) were purchased from Aldrich and used as received.

Polyoxometalates used here were all self-synthesized according to the literature procedure.[27−30] Typically used are a Keggin-type polyoxometalate (POM), $K_4[\beta\text{-}SiW_{12}O_{40}]\cdot 9H_2O$ (SiW_{12}),[27,28] a homopolyvanadate, $K_{12}V_{18}O_{42}$ (V_{18}),[29] and a rare earth element-containing polyoxometalate, $Na_9EuW_{10}O_{36}$ (EuW_{10}).[30]

Water used in all the experiments was distilled twice and had a resistivity higher than 18.2 MΩ·cm. Sodium chloride (NaCl), hydrochloric acid (HCl), manganese sulfate ($MnSO_4\cdot H_2O$, AR), ammonium bicarbonate (NH_4HCO_3, CP), citric acid ($C_6H_8O_7\cdot H_2O$, AR), and silver nitrate ($AgNO_3$, AR) were all purchased from the commercial market and used without further purification.

Template Preparation. $MnCO_3$ core particles with diameters of ∼1.8 μm were synthesized with the so-called poor solvent method.[31] Ethanol (0.5 mL) was added to a 99.5 mL solution containing 0.008 M $MnSO_4$ and 0.08 M NH_4HCO_3, and the mixture was stirred until the reaction is complete. The obtained white precipitates were isolated with centrifugation and dried at 60 °C under vacuum before further use. A more detailed description of the synthesis of $MnCO_3$ particles can be found elsewhere.[32]

PS core particles with diameters of ∼400 nm were synthesized according to the literature procedure.[33] In a 250 mL two-neck flask, 0.1 g of potassium persulfate and 0.11 g of sodium lauryl sulfate were dissolved in 70 mL of aqueous ethanol in which the ethanol:water volume ratio is 5:3. Then 4.5 mL of styrene was added under a nitrogen atmosphere and rapid stirring. The emulsion was subsequently heated to 70 °C to polymerize for 8 h. Prior to being used, the styrene was treated with 10% sodium hydroxide to remove the antipolymerizer.

Assembly of POMs into Microcapsules. Typically, 0.4 g of $MnCO_3$ particles was added to 10 mL of a 5×10^{-3} M citric acid solution, and then 10 mL of a 1 mg/mL PAH solution in 0.5 M NaCl (pH adjusted to ∼5.0 with 0.1 M HCl) was added under stirring to form a PAH/citrate shell.[34] Afterward, two (PSS/PAH) bilayers were assembled with the alternate adsorption of PSS and PAH monolayers starting from a PSS monolayer using a 2 mg/mL PSS solution and a 1 mg/mL PAH solution in 0.5 M NaCl. Subsequently, POM/PAH alternate adsorption was performed using a 5×10^{-3} M POM solution in 0.1 M NaCl and 1 mg/mL PAH in 0.5 M NaCl (pH ∼5.0). Following each adsorption step, nonadsorbed polyelectrolyte molecules or POMs were washed out with four repeated centrifugation−wash−redispersion cycles. After the formation of the $(PAH/PSS)_2(PAH/POM)_{10}PAH$ shell, the $MnCO_3$ core was dissolved in 0.1 M HCl, and the POM-based composite microcapsules were then obtained. To avoid the effects of HCl on the structure of V_{18} and EuW_{10}, when they were assembled into microcapsules, PS particles were used as templates, which were subsequently removed using acetone. Details about this assembly process are in the Supporting Information. A general assembly process was illustrated in Figure 1. The final products were collected and dried at 50 °C under vacuum for further measurement. A more detailed description of capsule preparation can be found elsewhere.[35−37]

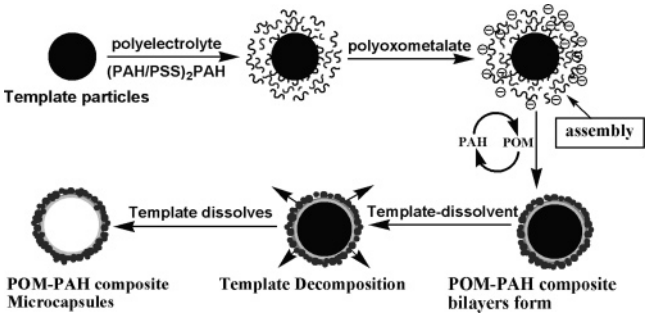

Figure 1. Illustration of the layer-by-layer assembly of polyelectrolyte and polymetalate onto template particles, decomposition of the core, and the formation of the POM-based composite microcapsules.

Characterizations. Scanning electron microscopy (SEM) images were obtained using a JEOL-2010 scanning electron microscope operated at 20 kV, and transmission electron microscopy (TEM) images were obtained using a JEM-2010 transmission electron microscope at an acceleration voltage of 200 kV. Samples dissolved in an ethanol/water mixture were treated with ultrasonic for 30 min to be well dispersed. Then one droplet of the suspension was absorbed on a copper grid (for TEM) or a glass wafer (for SEM), and the solvent was allowed to evaporate prior to measurement.

FTIR spectra were obtained using an Alpha Centaurt FTIR spectrophotometer with a KBr pellet. The wavenumber range is from 4000 to 400 cm^{-1}.

UV−vis absorption spectra were obtained using a 752 PC UV−vis spectrophotometer. Samples of hollow prepared microcapsules were dispersed in distilled water and filled in a quartz colorimetry cell.

XPS data were recorded using a VG ESCALAB MK II spectroscope with a Mg Kα (1253.6 eV) achromatic X-ray source. The vacuum inside the analysis chamber was maintained at 6.2×10^{-6} Pa when the analysis was being performed.

The photoluminescence study was carried out using a FL-2T2 instrument (SPEX) with a 450 W xenon lamp monochromatized by a double grating (1200 g/μm).

Results and Discussion

POM−PE composite microcapsules were produced with the layer-by-layer method. The drive force for the formation of the microcapsules should be traditional electrostatic attraction between oppositely charged species. As illustrated in Figure 1, POMs presumably form nanoaggregates in the presence of PAH, and these nanoaggergates bearing negative charges make the subsequent adsorption of cationic PAH possible and the layer-by-layer process successfully proceed. Similar phenomena have been observed when assembling POMs and polyelectrolytes onto flat quartz to construct composite films.[11−15] Such speculation

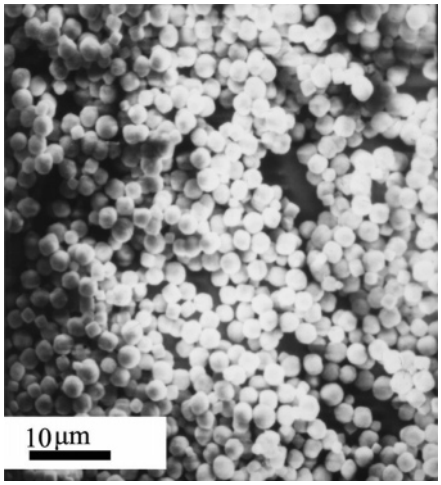

Figure 2. SEM image of $MnCO_3$ fresh particles, showing a mean diameter of ~1.8 μm.

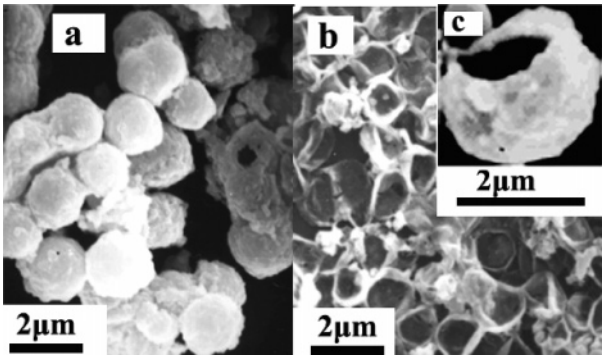

Figure 3. SEM images of the as-synthesized microcapsules: (a) the rough surface of the capsules, (b) broken capsules with a supported framework, and (c) an enlarged image of a microcapsule, showing the rough surface, the unevenness of the shell and the hollow structure, and the mean thickness of the shell.

was further verified by the morphology study. It was observed that connected nanoparticles are distributed in the shell of the hollow microcapsules as shown in typical TEM images in Figure 4c.

$MnCO_3$ template particles shown in the SEM image in Figure 2 have a round shape with an average diameter of ~1.8 μm. As seen in the SEM image in Figure 3a and the TEM image in Figure 4a, when the assembly process was completed, a rougher surface on the template particles was formed, and the mean diameter of these particles increased to ~2.3 μm, indicating the formation of bilayers on templates. The calculated thickness of the SiW_{12}−PE composite bilayers deposited on the template is ~250 nm, which is in agreement with the shell thickness of the microcapsules given in Figure 3c. The dried capsules reproduce the shape of the inorganic cores, and the POM nanoparticles tightly connected with PAH distributed in the shells (Figure 4b,c) prevent the capsules from collapse after drying, which is typical for empty polyelectrolyte capsules without an inorganic or organic interior frame.[33] However, the increased rigidity decreases the flexibility of the capsules; broken capsules were frequently seen especially from SEM, but their supported framework was maintained (Figure 3b). Meanwhile, the unevenness of the shell thickness was also observed (Figure 3c), which may be due to some occasional uneven deposition happening in the assembly process. Furthermore, comparing the micrographs of the finally produced microcapsules obtained from the assembly of PAH and different POMs, we can detect no obvious difference between the final micrographs of the

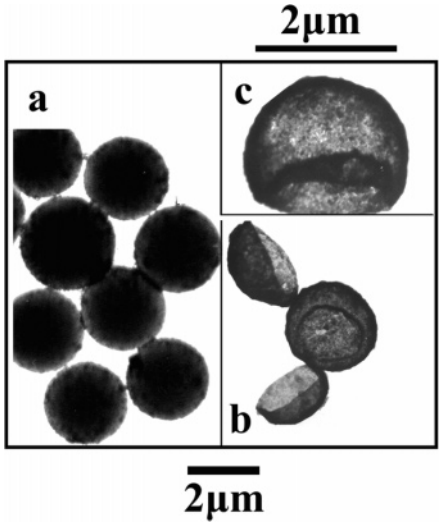

Figure 4. TEM images for the microcapsules: (a) the coated $MnCO_3$ particles with the core−shell structure, showing the presence of the bilayers, (b) hollow microcapsules, and (c) an enlarged image of a hollow capsule, showing the presence of tightly connected particles on the shell.

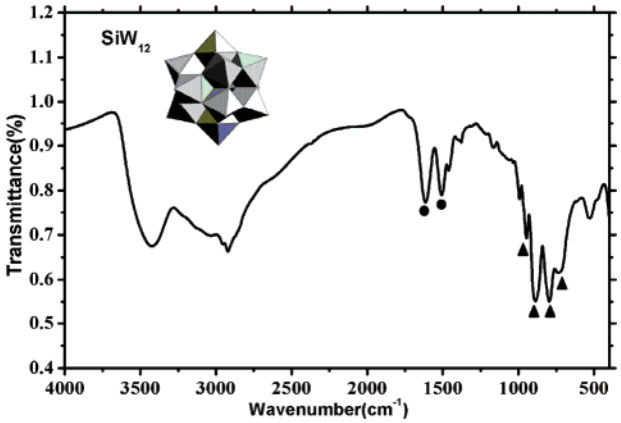

Figure 5. FTIR spectrum of the hollow capsules with the SiW_{12}−PAH composite as the shell (filled triangles indicate the peaks ascribed to SiW_{12}, and filled dots indicate the peaks ascribed to NH_3^+). The inset is the structure of SiW_{12}^{4-}.

microcapsules except some small variations which can be readily attributed to uncertain factors in the experimental operations (Figure S1 of the Supporting Information).

The FTIR spectrum of hollow microcapsules with the SiW_{12}−PAH complex as a shell component is given in Figure 5. Four characteristic peaks of POM [737.92 cm^{-1} ascribed to ν(W−Oc−W), 792.25 cm^{-1} ascribed to ν(W−Ob−W), 887.46 cm^{-1} ascribed to ν(W═Od), and 946.60 cm^{-1} ascribed to ν(Si−Oa) (where Oa is the oxygen of the central tetrahedral, Ob the bridged oxygen of two octahedra sharing a corner, Oc the bridged oxygen sharing an edge, and Od the terminal oxygen)] attest to the presence of POM in the shell.[27] All the peaks experience a slight shift to lower wavenumbers. This may be due to the interaction between SiW_{12} and PAH. The well-resolved bands at 1615.12 and 1508.45 cm^{-1} ascribed to the asymmetry stretching vibration and symmetry distorting vibration of NH_3^+, respectively, 1378.38 cm^{-1} ascribed to the symmetry distorting vibration of $-CH_3$, 3425.37 cm^{-1} ascribed to the N−H stretching vibration, and bands ranging from 2920 to 3033 cm^{-1} ascribed to the hydrogen bonding between molecules or C−H vibration all verify the presence of PAH. The same phenomena appear in all the other kinds of hollow microcapsules, and their FTIR spectra show similar patterns,

verifying the commonness of POM−PAH composite microcapsules (Figure S2 of the Supporting Information).

In a comparison of the UV−vis absorbance spectrum of a pure $K_4[\beta\text{-}SiW_{12}O_{40}]\cdot 9H_2O$ aqueous solution and that of SiW_{12}−PAH-based hollow microcapsules, two characteristic absorbance bands at 200−210 and 260−300 nm corresponding to oxygen → tungsten charge transfer (CT) appearing in Figure S3(a) of the Supporting Information also verify the presence of POM in the shell. The interaction between POM and PAH, whose characteristic peak should appear at 195 nm, likely accounts for the broadening and the intensity change of the two bands. The same phenomenon was also observed when collecting the UV−vis spectra of those capsules with other POMs [Figure S3(b−d) of the Supporting Information].

An XPS study of a sample of the SiW_{12}−PAH composite microcapsules shows the state of element W. Two characteristic binding energy peaks of W ($4f_{7/2}$, 35.2 eV; $4f_{5/2}$, 36.6 eV)[15] show that W maintains its original valence (VI) (Figure S4 of the Supporting Information). Such a result combined with the fact that Si cannot experience redox under the current mild conditions indicates that in the assembly process, no redox process occurs. The pH values of the PAH and 0.1 M HCl solutions that were used are around 5.0 and 2.0, respectively, values at which SiW_{12} cannot experience polymerization or degradation. Such a fact combined with the expected Si:W ratio of approximately 1:12 calculated from XPS data attests to the maintenance of the POM structure, and thus the original properties of the POMs assembled into microcapsules. For different POMs (usually stable at pH <7.0), the pH value of the polyelectrolyte solutions can be carefully adjusted so as to guarantee their stability, and the stability of polyelectrolytes (stable under acidic conditions) can also be maintained. The same XPS results were also obtained when studying capsules with other POMs as a component.

The microcapsules obtained here also exhibit their thermal stability in a manner different from those common polyelectrolyte microcapsules which are only stable at temperatures below 80 °C.[38] A water dispersion of the composite microcapsules was heated to boil for 1 h, and no obvious difference in their morphology can be seen under a microscope. Meanwhile, their FTIR, UV−vis, and XPS spectra also show no variance, showing the higher thermal stability of the POM-based microcapsules. However, the UV−vis spectrum of the supernatant also shows the characteristic absorption bands of POM, indicating partial dissolution of POMs into water.

Substituted Keggin type polyoxometalates, for example, $K_6[SiCoW_{11}O_{40}H_2]\cdot 14H_2O$, $K_6[SiNiW_{11}O_{40}H_2]\cdot 14H_2O$, and $K_6[GeCoW_{11}O_{40}H_2]\cdot 14H_2O$, were also assembled into microcapsules, and the study of their above-mentioned characteristics gives similar results (Figure S1−S3 of the Supporting Information).

Polyoxometalates bear unique electronic characteristics. The incorporation of transition metals into their framework provides a source of weakly attached electrons which can be transferred to other compounds, and thus can easily induce the proceeding of reduction. In view of this, $K_{12}V_{18}O_{42}$ homopolyoxovanadate was assembled into microcapsules to study its effect on the reduction of Ag^+. To prevent the effect the acid may have on V_{18}, PS particles were used as templates. At room temperature, after addition of 5 mL of an 18 mg/mL $AgNO_3$ solution to a 10 mL $(PAH/V_{18})_{10}$ composite microcapsule dispersion dropwise with a dark blue color under stirring, the mixture quickly became rufous, indicating the formation of Ag clusters which have a red color. The UV−vis spectrum of a water dispersion of the

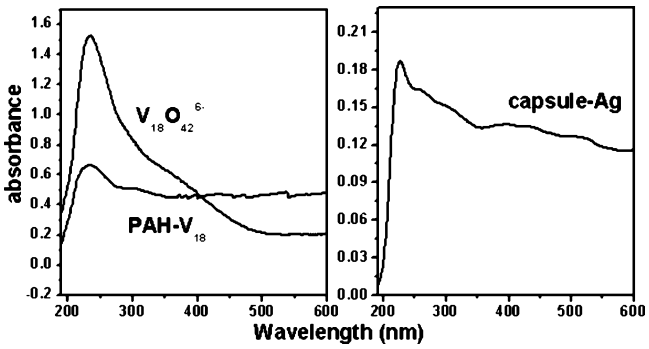

Figure 6. UV−vis spectra of a homopolyoxovanadate $K_{12}V_{18}O_{42}$ water solution, water dispersion of $V_{18}O_{42}$−PAH composite microcapsules, and water dispersion of the capsules when Ag^+ reduction was performed.

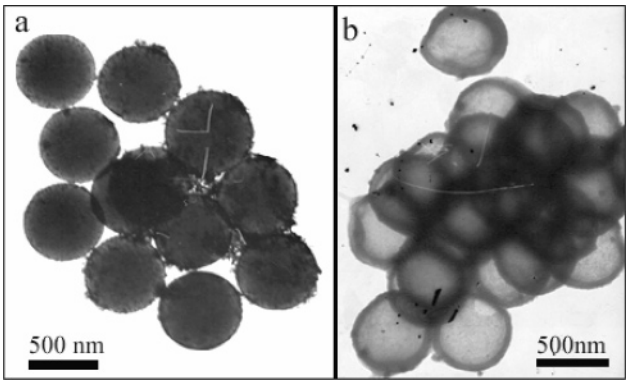

Figure 7. TEM images for (a) PEI−$V_{18}O_{42}$−Ag composite capsules with PS template particles as cores and (b) PEI−$V_{18}O_{42}$−Ag composite capsules.

Ag-based capsules in Figure 6 shows two broad absorption bands at 310 and 390 nm, which can be attributed to the absorption of smaller Ag_n clusters ($n = 2-12$)[39−43] and a collective oscillation of the electron gas in the nanometer-scale particles, respectively (plasmon absorption).[39,40]

Furthermore, TEM images of the final products show microcapsules with a denser surface, verifying the deposition of Ag nanoparticles onto their shells. Figure 7 gives the typical TEM images of the finally obtained PAH−V_{18}−Ag composite capsules with PS template particles as cores and those hollow ones with PAH−V_{18}−Ag composite shells.

The silver-coated microcapsules may prove to be useful in catalysis.[44] Such an experiment provides a way to apply POM-based microcapsules. When other kinds of POMs bearing redox activity are incorporated into microcapsules, expected redox processes can be performed preferentially on the shell, thus realizing the in situ synthesis of materials and the development of catalysts.

It has been reported in the literature that when photoluminescent POMs were assembled onto flat quartz, functional films bearing photochromic[14] properties can be yielded. Here, PAH/EuW_{10} bilayers were successfully transferred to microcapsules, and photoluminescent microcapsules were obtained. Figure 8 gives the photoluminescence spectrum of the as-obtained $(PAH/EuW_{10})_{10}$ microcapsules. At room temperature, when $[EuW_{10}O_{36}]^{9-}$ is excited in intense UV bands corresponding to oxygen−tungsten transitions within the $[EuW_{10}O_{36}]^{9-}$ "ligand", or in weak bands corresponding to f−f excited states of the Eu^{3+} ion in the visible region, weak luminescence derived from $^5D_0 \rightarrow {}^7F_J$ ($J \sim 0$, 1, 2, 3, and 4) transitions can be observed.[45−47] They are two $^5D_0 \rightarrow {}^7F_1$ transitions, one $^5D_0 \rightarrow {}^7F_2$ transition, one $^5D_0 \rightarrow {}^7F_3$ transition, and two $^5D_0 \rightarrow {}^7F_4$ transitions. As

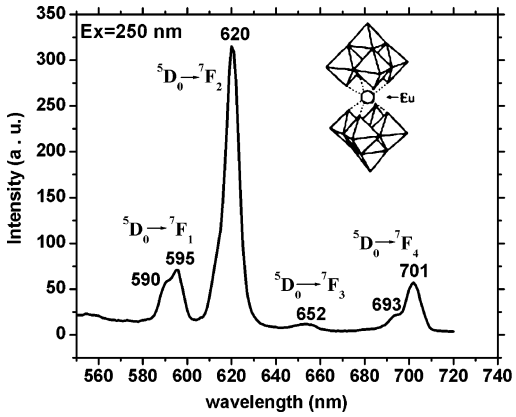

Figure 8. Photoluminescence spectrum of $(PAH/EuW_{10})_{10}$ microcapsules. The positions of $^5D_0 \rightarrow {}^7F_J$ ($J \sim 0$, 1, 2, 3, and 4) emission bands are indicated in wavelength (nanometers). The inset is the structure of $[EuW_{10}O_{36}]^{9-}$.

shown in Figure 8, the fluorescence behavior of the $(PAH/EuW_{10})_{10}$ microcapsules is essentially identical to that of the EuW_{10} solid sample we prepared, except the relative intensities and the bandwidths. (Because the EuW_{10} used here is self-synthesized, and some imperfection may exist in the structure, the photoluminescence spectrum obtained here is slightly different from that of the traditional EuW_{10}.) This confirms that $[EuW_{10}O_{36}]^{9-}$ retained its structure when assembled into the shell of microcapsules. That is to say, $[EuW_{10}O_{36}]^{9-}$ polyanions can stably exist in microcapsules, and the dominant interaction between EuW_{10} and PAH is indeed electrostatic attraction, with the original coordination of Eu^{3+} maintained. However, because of the low content of EuW_{10} present in the microcapsules, the fluorescence intensity is weak, so the fine structure in the bilayers is not revealed. The occurrence of photoluminescent activity in microcapsules provides potential for creating luminescent capsules with POMs as a component. Furthermore, their functions can be modified by adjusting the types of POMs, and the thickness, composition, and structure of the bilayers.

The feasibility of assembling POMs with different polyelectrolytes, for example, poly(ethylenimine) (PEI), onto different kinds of templates, for example, PS and SiO_2 latex, was also investigated, and similar results were obtained. Such a result provides insight into the combination of various POMs and different cationic polyelectrolytes in a capsule environment in achieving various expected functions.

Conclusions

Different types of polyoxometalates were assembled into the shell of microcapsules. Study results demonstrate that POMs form nanoparticles in the presence of polyelectrolytes, and these particles connected with polyelectrolyte are uniformly distributed in the shells and help the composite capsules withstand drying. Furthermore, the functions of polyoxometalates were maintained in the microcapsules, and a new environment applicable for further use can be constructed. Introducing polyoxometalates into microcapsules may provide a new avenue for the development of polyoxometalate functional materials and the interconnection of subjects, for example, medicine and inorganic chemistry.

Acknowledgment. Financial support for this work was provided by the National Natural Science Foundation of China (Grant 20371011).

Supporting Information Available: Synthetic procedures for the capsules fabricated using PS as templates; TEM and SEM images and FTIR spectra for microcapsules with substituted keggin-type polyoxometalates as a component; UV-vis spectra for capsules with SiW_{12} and substituted keggin-type polyoxometalates as a component and their corresponding parent polyoxometalate water solutions; the XPS spectrum for element W present in SiW_{12} capsules. This material is available free of charge via the Internet at http://pubs.acs.org.

References and Notes

(1) Mizuno, N.; Misona, M. *Chem. Rev.* **1998**, *98*, 199.
(2) Ben-Daniel, R.; Weiner, L.; Neumann, R. *J. Am. Chem. Soc.* **2002**, *124*, 8788.
(3) Izumi, Y.; Urabe, K.; Onaka, M. *Zeolite, Clay, and Heteropoly Acid in Organic Reactions*; VCH: Weinheim, Germany, 1992.
(4) Lomakina, S. V.; Shatova, T. S.; Kazansky, L. P. *Corros. Sci.* **1994**, *36*, 1645 and references therein.
(5) Katsoulis, D. E. *Chem. Rev.* **1998**, *98*, 359.
(6) Sadakane, M.; Steckhan, E. *Chem. Rev.* **1998**, *98*, 219.
(7) Keïta, B.; Nadjo, L. *Mater. Chem. Phys.* **1989**, *22*, 77.
(8) Rong, C.; Anson, F. C. *Anal. Chem.* **1994**, *66*, 3124.
(9) Rong, C.; Anson, F. C. *Inorg. Chim. Acta* **1996**, *242*, 11.
(10) Klemperer, W. G.; Wall, C. G. *Chem. Rev.* **1998**, *98*, 297.
(11) Moriguchi, I.; Fendler, J. H. *Chem. Mater.* **1998**, *10*, 2205.
(12) Kurth, D. G.; Volkmer, D.; Ruttorf, M.; Richter, B.; Müller, A. *Chem. Mater.* **2000**, *12*, 2829.
(13) Liu, S. Q.; Kurth, D. G.; Bredenkötter, B.; Volkmer, D. *J. Am. Chem. Soc.* **2002**, *124*, 12279.
(14) Wang, Y. H.; Wang, X. L.; Hu, C. W.; Shi, C. S. *J. Mater. Chem.* **2002**, *12*, 703.
(15) Jiang, M.; Wang, E. B.; Kang, Z. H.; Lian, S. Y.; Wu, A. G.; Li, Z. *J. Mater. Chem.* **2003**, *13*, 647.
(16) Jiang, M.; Wang, E. B.; Xu, L.; Kang, Z. H.; Lian, S. Y. *J. Solid State Chem.* **2004**, *177*, 1776.
(17) Kang, Z. H.; Wang, E. B.; Jiang, M.; Lian, S. Y.; Li, Y. G.; Hu, C. W. *Eur. J. Inorg. Chem.* **2003**, *2*, 370.
(18) Kang, Z. H.; Wang, Y. B.; Wang, E. B.; Lian, S. Y.; Gao, L.; You, W. S.; Hu, C. W.; Xu, L. *Solid State Commun.* **2004**, *129*, 559.
(19) Kang, Z. H.; Wang, E. B.; Jiang, M.; Lian, S. Y. *Nanotechnology* **2004**, *15*, 55.
(20) Bu, W. F.; Li, H. L.; Sun, H.; Yin, S. Y.; Wu, L. X. *J. Am. Chem. Soc.* **2005**, *127*, 8016.
(21) Caruso, F. *Chem.—Eur. J.* **2000**, *6*, 413.
(22) Caruso, F.; Caruso, R. A.; Möhwald, H. *Science* **1998**, *282*, 1111.
(23) Shchukin, D. G.; Ustinovich, E.; Sviridov, D. V.; Lvov, Y. M.; Sukhorukov, G. B. *Photochem. Photobiol. Sci.* **2003**, *2*, 975.
(24) Shchukin, D. G.; Shutava, T.; Shchukina, E.; Sukhorukov, G. B.; Lvov, Y. M. *Chem. Mater.* **2004**, *16*, 3446.
(25) Zhao, Q. H.; Gao, C. Y.; Shen, J. C.; Li, Y.; Zhang, X. B. *Macromol. Rapid Commun.* **2004**, *25*, 2014.
(26) Radtchenko, I. L.; Sukhorukov, G. B.; Leporatti, S.; Khomutov, G. B.; Donath, E.; Möhwald, H. *J. Colloid Interface Sci.* **2000**, *230*, 272.
(27) Kurth, D. G.; Volkmer, D. In *Polyoxometalate Chemistry*; Pope, M. T., Müller, A., Eds.; Kluwer: Dordrecht, The Netherlands, 2001; p 301.
(28) Rocchiccioli-Deltcheff, C.; Fournier, M.; Franck, R.; Thouvenot, R. *Inorg. Chem.* **1983**, *22*, 207.
(29) Müller, A.; Penk, M.; Rohlfing, R.; Krickemeyer, E.; Doring, J. *Angew. Chem., Int. Ed.* **1990**, *29*, 926.
(30) Peacock, R. D.; Weakley, T. J. R. *J. Chem. Soc. A* **1971**, 1836.
(31) Antipov, A.; Shchukin, D.; Fedutik, Y.; Zanaveskina, I.; Klechkovskaya, V.; Sukhorukov, G.; Möhwald, H. *Macromol. Rapid Commun.* **2003**, *24*, 274.
(32) Hamada, S.; Kudo, Y.; Okada, J.; Kano, H. *J. Colloid Interface Sci.* **1987**, *118*, 356.
(33) Zhang, J. H.; Chen, Z.; Wang, Z. L.; Zhang, W. Y.; Ming, N. B. *Mater. Lett.* **2003**, *57*, 4466.
(34) Sukhorukov, G. B.; Brumen, M.; Donath, E.; Möhwald, H. *J. Phys. Chem. B* **1999**, *103*, 6434.
(35) Shchukin, D. G.; Sukhorukov, G. B.; Möhwald, H. *Angew. Chem., Int. Ed.* **2003**, *42*, 4472.
(36) Sukhorukov, G. B.; Donath, E.; Davis, S.; Lichtenfeld, H.; Caruso, F.; Popov, V. I.; Möhwald, H. *Polym. Adv. Technol.* **1998**, *9*, 759.
(37) Sukhorukov, G. B. Designed Nano-Engineered Polymer Films on Colloidal Particles and Capsules. In *Novel Methods to Study Interfacial Layers*; Mobius, D., Miller, R., Eds.; Elsevier Science: Amsterdam, 2001; p 384.
(38) Gao, C. Y.; Leporatti, S.; Moya, S.; Donath, E.; Möhwald, H. *Chem.—Eur. J.* **2003**, *9*, 915.

(39) Henglein, A.; Linnert, T.; Mulvaney, P. *Ber. Bunsen-Ges.* **1990**, *94*, 1457.
(40) Mostafavi, M.; Keghouche, N.; Delcourt, M.-O.; Belloni, J. *Chem. Phys. Lett.* **1990**, *167*, 193.
(41) Murphy, C. J.; Jana, N. R. *Adv. Mater.* **2002**, *14*, 80.
(42) Gutierrez, M.; Henglein, A. *J. Phys. Chem. B* **1993**, *97*, 11368.
(43) Mostafavi, M.; Keghouche, N.; Delcourt, M.-O. *Chem. Phys. Lett.* **1990**, *169*, 81.
(44) Antipov, A. A.; Sukhorukov, G. B.; Fedutik, Y. A.; Hartmann, J.; Giersig, M.; Möhwald, H. *Langmuir* **2002**, *18*, 6687.
(45) Ballardini, R.; Mulazzani, Q. G.; Venturi, M.; Bolletta, F.; Balzani, V. *Inorg. Chem.* **1984**, *23*, 300.
(46) Stillman, M. J.; Thomson, A. J. *J. Chem. Soc., Dalton Trans.* **1976**, *12*, 1138.
(47) Blasse, G.; Dirksen, G. J.; Zonnevijlle, F. J. *J. Inorg. Nucl. Chem.* **1981**, *43*, 2847.